

Architectonics of the Crown Part of the Tooth of Humans and Mammals

VM Zolotarev*

National Research University of Information Technology, Mechanics and Optics, St. Petersburg, Russia

***Corresponding Author:** VM Zolotarev, National Research University of Information Technology, Mechanics and Optics, St. Petersburg, Russia.

Received: November 09, 2022

Published: January 06, 2023

© All rights are reserved by **VM Zolotarev.**

Abstract

By methods of polarization optical microscopy and electrometry, a study of the structural organization of dentin tubes on the grindings of the crown part of the human and pig tooth was carried out. It is shown that in the region of the tubercles of the tooth, dentin tubes are a bundle in the form of a cone, the top of which is directed to the region of the tooth pulp, and the center of the base of the cone faces the zone of the apex of the tubercle. In individual specimens of teeth for crossed polarizers in the region of the tubercles of the tooth, pictures in the form of «Maltese crosses» surrounded by concentric circles were observed. By methods of mathematical modeling within the framework of geometric (beam) and wave optics, calculations were carried out for a number of compositions from the tube system and thereby the interpretation of the data obtained was substantiated. The influence of the mutual arrangement of tubes on their ability to exchange light energy is shown. The substantiation of the color paintings obtained for the sections of the molar along and across the tubes is given. The information obtained for the structure of the crown shape of the human molar tooth is compared with similar teeth of a pig and some mammals.

Keywords: Human Molar Tooth; Polarization Optical Microscopy; Spectroscopy and Electrometry

Introduction

The optical properties of tooth dentin can be described as «a set of two subsystems consisting of a diffusely scattering medium (matrix) and tubules» permeating this medium and diverging in a fan from the pulp area in the direction of the dentino-enamel compound (DES) [1,2]. In this case, they usually proceed from the assumption that in a thin layer of grinding, the tubes are «located parallel to each other and are more or less evenly distributed along the cross-section of the tooth.» At the same time, there are currently a number of works indicating the anisotropic structure of dentin [3-5].

Dentin consists of three main components: organic matter based on collagen (matrix), minerals (mainly hydroxyapatite), and dentin tubes that permeate the entire volume of dentin [6,7]. The

features of the propagation of light radiation in dentin were first drawn attention to in the work [6]. According to [6], the tubules work as light guides and light propagates inside the tubes by both Fresnel reflection from the inner surface of the tube and in the layer limited by the outer and inner diameter of the tubes, i.e. in the layer of peritubular dentin. The ability of light to propagate through tubes that perform the function of fibers is noted, and a number of works have shown [4,6] that tooth grinding acts like an optical element of a focon, having the ability to increase or decrease the image of the test object depending on which side the grind comes into contact with the object. The gap between the inner wall of the tube is filled with dentin fluid, which is close in composition to plasma. Dentin, which occupies the space between the tubes, is called intertubular, and dentin that forms the walls of the tubes is called peritubular. Peritubular dentin differs from intertubular dentin in its high content of mineral components (40% more).

An increase in the mineral component leads to an increase in the refractive index, therefore, for different components of dentin, the ratio is performed: peritubular > intertubular dentin > fluid. It is important to note that the axis-c of the HAP crystals, which coincides with their optical axis, is oriented parallel to the axis of the tube, so the tubules also have the properties of a single-axis crystal [8]. Figure 1 shows the scheme of the molar tooth (Figure 1a) and the scheme of the dentin tube with the odontoblast cell and the nerve fiber in the wall of the tubule (Figure 1b). Nerve fibers are present only in part of the dentin tubes. In the crown area, the proportion of such tubes is 0.005-8%, and in the region of the horns, the pulp reaches 25% for molars. It is believed that the nerve fibers in the tubules control the activity of odontoblasts, i.e. transmit impulses from the nerve centers to the working organs [7].

Figure 1: a: Diagram of the structure of the molar tooth. 1- enamel, 2- dentin, 3- pulp, 4- dentino-enamel layer. 5- grinding, P1 and P2 - planes of grinding. b-Diagram of a dentin tube with a nerve fiber see the view on the arrow.

In modern physical literature in recent years, considerable attention has been paid to theoretical and applied issues related to the use of optical methods for the study of biological objects [9-13]. However, according to reviews [14,15], these studies are predominantly focused on the study of ophthalmology tasks, i.e. relative to transparent eye media or dissipating cell suspensions. At the same time, the study of highly dispersing anisotropic media, such as tooth dentin, encounters considerable difficulties [15-17], although attempts to apply optical methods to study it have increased markedly in recent years [1-2,18]. The study of the optical properties of the human tooth is important for a number of

fundamental problems of morphology and anthropology [7,14-17], as well as for solving applied problems of dentistry and materials science, in particular for developing requirements for restoration materials from the standpoint of the necessary correspondence of their aesthetic properties to the optical characteristics of an individual tooth. Studies of the structure of the tooth are of paramount importance for the formation of a physical model of the tooth, which is the basis for building an adequate initial model for computer processing of data by various methods of tomography, in particular, optical diffuse tomography.

Optical [1-3,18-20] and spectral [5,8] methods are widely used to study the structure of dentin, as well as to diagnose dental diseases and in particular caries [18-20]. In works on light scattering, it is believed [2,14] that the optical properties of dentin can be modelly described as “a combination of two subsystems consisting of a diffusely scattering medium (matrix) and tubes” permeating this medium and diverging in a fan from the pulp region in the direction of the dentino-enamel compound (DES). In all works modeling the optical properties of dentin, it is assumed that in a thin layer of grinding, the tubes are “located parallel to each other and more or less evenly distributed along the tooth cross-section.” However, in the works [3,20] there were differences in the propagation of light inside the tooth, depending on which area of the crown of the tooth to direct a narrow beam of He-Ne laser. These observations indirectly indicate a more complex anisotropic structure of dentin. Therefore, it was important to try to detect and systematically study these structural features of the dentin structure in the local areas of the crown part of the tooth by more subtle optical methods.

The structure of the hard tissues of the tooth according to the data

Optical measurements

The tubes according to [18] work as light guides and light can propagate both inside the tubes by mirror reflection from the inner surface of the tube, and in the layer limited by the outer and inner diameter of the tubes. However, these works [6,19,20] do not address the reasons why the grinds in different zones differ in the ability to zoom in and out of the image of the test object. In this regard, it should be noted that further research aimed at clarifying the structural features of the bio tissues of the tooth, which can be studied using optical methods, are the key to advancing the study

of the architectonics of dentin in the crown part of the tooth. These data should be used as the basis for new diagnostic and therapeutic hardware methods, as well as instrumental means, for example, X-ray and optical diffuse tomography [9,12].

Physical properties

The tooth consists of dentin covered in the crown part with enamel. The enamel is formed by enamel prisms, which consist of densely packed hexagonal crystals of hydroxyapatite (HAP)- $\text{Ca}_{10}(\text{PO}_4)_6(\text{OH})_2$ [21]. The length of the crystals varies from 100 to 1000 nm, thickness 25-40 nm, width 40-90 nm. The average refractive index of apatite is $n = 1.632 \div 1.642$. The diameter of the tubules decreases in the direction from the pulp, where it is 2-3 μm , in the direction of the dentino-enamel junction (0.5-1 μm). The birefringence of HAP crystals of different deposits is $\Delta n = n_e - n_o \approx - (0.003 \div 0.005)$. On the basis of small HAP crystals, larger formations are formed – enamel prisms, which have a higher hardness compared to HAP crystals. Individual crystals in prisms are ordered – optical axes-S the HAP crystals near the central part of the prism are almost parallel, and as they shift to the periphery of the prism, the lengths of the HAP crystals begin to deviate more and more, forming significant angles with the prism axis. The diameter of enamel prisms is 3-5 μm , they have an S-shaped bend and are oriented mainly perpendicular to the surface of the tooth. The spaces between prisms are filled with protein, the refractive index of which is about $n = 1.45$, and the thickness of the corresponding layers is 1-2 nm.

Dentin has a more complex structure and consists of three main components: organic matter based on collagen (matrix), minerals (mainly hydroxyapatite), and dentin tubes that penetrate the entire volume of dentin. Dentin has much smaller sizes of HAP crystals than enamel. The length of the crystals varies from 10 to 90 nm with an average length of 36 nm; the thickness is 4-17 nm at an average size of 10 nm. The matrix is formed from disordered fibrils fibers with a diameter of 50-150 nm and forms a framework filled with small HAP crystals that form larger globular globules. Collagen molecules in fibrils have a chain length of 280 ± 1.5 nm at a molecular weight of $\sim 360,000$. The number of tubes in dentin, according to different authors, ranges from $15-65 \times 10^3/\text{mm}^2$ - average values of $35 \times 10^3/\text{mm}^2$. The diameter of the tubes decreases in the direction from the pulp, where it is 2-3 μm , in the direction of the dentino-enamel

compound (0.5-1 μ). The gap between the inner wall of the tube is filled with a liquid that is close in composition to blood plasma. Since cellular structures contain a lot of water, the refractive index of the inner part of the tubes is close in size to water ($n = 1.33$). The tubules depart from the pulp of the tooth and fan out towards the border of the dentino-enamel junction, Figure 1. The thickness of the peritubular dentin layer increases in the direction from the pulp (44 nm) to the DES, where it reaches 750 nm. With the aging of the tooth, the tubule channels become clogged with HAP crystals, which leads to the mineralization of dentin. It is important to note that the axis-S of the HAP crystals, which coincide with the optical axis, is oriented in the peritubular dentin parallel to the axis of the tubule. At the same time, their lengths will be predominantly oriented along the axis of the NAR. tubes, i.e. tubes will also have the properties of a single-axis crystal. This information is important for subsequent judgments about the role of tubes in the transport of light radiation.

Model calculations of optical properties for a number of configurations of dentin tubes

Geometric model

It is known that optical research methods, such as the interference-polarization method, have high resolution and sensitivity, and thus can provide the most detailed information about the structure of the object. The choice of method was based on the initial model adopted in the literature to describe the optical properties of dentin, as “a combination of two subsystems consisting of a diffusely scattering medium and tubes”.

The use of polarized light in the polarizer-dentin-analyzer measurement scheme was supposed to reduce the scattered component, i.e. to partially suppress the diffuse component and thus raise the contrast of the observed interference pattern, which is determined by the optical properties of the tubes. Within the framework of beam optics, we will analyze the properties of relatively thick anisotropic fibers in which the diameter D significantly exceeds the length of the light wave [8,22]. This approximation allows us to consider in the beam approximation a system of fibers distributed in a homogeneous optically less dense medium. Suppose that the fibers are distributed in a transparent medium (matrix) having a refractive index of λ, n_m , and have the

properties of uniaxial crystals ($n_{kr}, \Delta n_{max} = n_e - n_o$) in which the optical axis coincides with the axis of the fiber. Fibers can be solid or tubular. The fiber system when, $n_{kr} > n_m$, when illuminated by a beam of light from the side of the fiber ends is able to transport light along the fiber using the phenomenon of complete internal reflection.

As a result, a beam of linearly polarized light when passing through an anisotropic fiber will divide into two orthogonal components S_o and S_e , which at the output of the fiber will have some phase difference. The resulting value of the phase difference depends on the length of the fiber, the angle of incidence of the light beam at the medium-fiber boundary, and the values of the relative refractive indices $n_1 = n_m/n_{kr}$ and $n_2 = n_m/n_{kr}$, of the magnitude of the birefringence Δn_ϕ and the number of reflections N .

The phase difference between the rays S_o and S_e during the passage of the fiber for its principal sections can be represented as an additive sum [8];

$$\delta = \delta_1 + N\delta_2 \text{----- (1)}$$

In this approximation, component δ_1 of the phase difference due to the passage of light in the thickness of the sample and component δ_1, δ_2 due to the complete internal reflection of the rays S_o and S_e . The value δ_1 can be calculated for the main cross-sections of the fiber from the equation:

$$\delta_1 = (\delta_e - \delta_o) = \frac{2\pi}{\lambda} d(n'_e - n'_o), \text{----- (2)}$$

Where $\delta_e - \delta_o$ is the phase difference between the rays S_o and S_e , resulting from the passage of light of the anisotropic plate, d - the thickness of the plate, n'_e and n'_o - refractive indices for the arbitrary direction of the rays S_o and S_e in the fiber, respectively. Optical dispersion, n_λ for the rays S_o and S_e does not make significant adjustments to the calculation of the phase difference in equation (2) and is not further taken into account.

Another component δ_2 , due to the complete internal reflection of the rays S_o and S_e from the fiber boundary can be calculated from the equation;

$$\frac{1}{2} \delta_2 = \frac{1}{2} (\delta_e - \delta_o) = \frac{\cos \varphi \sqrt{\sin^2 \varphi - n^2}}{\sin^2 \varphi} \text{----- (3)}$$

The corresponding value must be multiplied by factor N -number of light reflections in the fiber. If the fiber is tubular, then for its main

sections, it should be borne in mind that $N/2$ reflections occur at the boundary with the relative refractive index $n_1 \equiv n_m/n_{kr}$ and the other part of the reflections, $N/2$ occurs at the boundary where $n_2 \equiv n_m/n_{kr}$. The smallest value of the limiting critical angle $\sin \phi_{TR} = n_1$, for which light passes inside the tubular fiber is determined by the value n_1 .

If we take a sample within which the fibers conically diverge from the center of the grind to the edges of the sample in the direction of the upper plane, such a system will detect a radial dependence of the phase difference of the rays S_o and S_e at the exit of a single fiber. If the fibers are symmetrically deviated from some axis located in the center of the sample, then the corresponding changes in the phase relationships between the rays S_o and S_e propagating in each individual fiber will also follow the rules of radial symmetry. In general, the rays coming out of individual fibers will be elliptically polarized. The polarization form of such rays will depend on the specific location in the aggregate fiber bundle of each individual fiber. It depends on the parameters: $d, \phi, n, \Delta n, N$ and the azimuth of polarization of incident light. As a result, when illuminating the sample with a monochromatic parallel beam of linearly polarized light, if the polarizer and analyzer are deployed at an angle 90° , it is possible to observe in the center of the sample a figure in the form of a «Maltese cross» around which light and dark concentric rings are located, figure 2 [8].

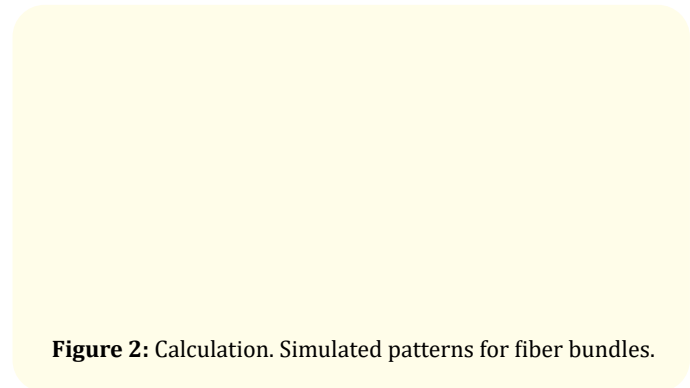


Figure 2: Calculation. Simulated patterns for fiber bundles.

Calculation for axisymmetric beam of anisotropic fibers in fine grinding (thickness 1mm): Different calculation conditions: thickness of the sample (a, b), angular width of the fibre bundle alignment (c, d), angle of inclination of the bundle axis (e, f), and outer and inner diameters of tubular fibre (g, h).

Experiment (right): k-conoscopic pattern for a single-axis massive crystal carved perpendicular to the o.o. (thickness 1 cm).

The first light ring from the center of the cross in Figure 2 corresponds to the phase difference 2π arising after the passage of light directly through the optical fiber and the phase difference π which is associated with the experimental conditions, i.e. with crossed position of polarizer and analyzer. The first dark ring corresponds to the phase difference of $2\pi + \text{etc.}$ Light rings, as in the case of the passage of light through a single crystal, have the greatest brightness in the directions located along the diagonals of the dark cross. The appearance of a dark cross is due to the fact that in the corresponding areas interference pattern each ray passing through a separate fiber makes oscillations in the plane of oscillations of one of the polarizers (nikolas). Such rays propagating along the main section of the fiber do not undergo double refraction and therefore are not passed by the subsequent polarizer.

Thus, the formation of the cross and the system of light and dark rings around it is associated with the interference of polarized light during the passage of a system of anisotropic fibers ordered according to the law of axial symmetry [22-24]. If the axis of symmetry of the bundle of divergent fibers is perpendicular to the surface of the sample, then the branches of the dark cross will coincide with the directions of oscillations of the electric vector of the light wave in the polarizer and analyzer. Light and dark rings have the shape of a circle since for these directions interfering rays have equal phase shifts. Taking into account the azimuth of the plane of polarization of incident light, shows that the influence of this factor will be most noticeably manifested in the direction of the diagonals of quadrants enclosed between the intersections of dark lines that form crosses. This influence will be expressed in the depolarization of the outgoing beams, as a result of which the dimming of light by the analyzer in this direction will not be complete. Therefore, in this area of the quadrants of the cross, the calculation does not fully coincide with the experiment.

The influence of the structural organization of the tubules on the optical properties of the tooth

The calculation of interference-polarization patterns of model systems in the form of a set of tubes of different structural organization should be carried out taking into account: the lighting conditions of the grind, the optical properties of the matrix and

hollow tubes, different thicknesses of the grind, different ratios of the external and internal diameter of the tubes, the angle of inclination of the tubes, the angle of alignment (divergence) of the tubes. To this end, software has been developed that allows, in a radial approximation, to perform calculations of interference-polarization patterns formed after passing through a set of tubes in tooth grinds [25]. The model takes into account the optical properties of the environment (matrix), the fiber itself, its shape, size, as well as the inclination of the fiber. It is possible to transform the model into a system of tubes with a conical stroke of the inner hole.

Interference patterns obtained with the help of the developed software, arising from the passage of light of a system of anisotropic tubular fibers ordered according to the law of axial symmetry, are given in figure 2. During the simulation, some conditions and parameters of the composite system are fixed: $D_n, D_m, \phi, \phi_1, d, n_{kr} = 1.59$ [26], $n_m = 1.45-1.5$ [1,26], $n_w = 1.33$ [1,21,26]. As variables, the thickness of the sample (a, b), the angular width of the fibre bundle flap (c, d) and the angle of inclination of the axis the bundle (e, f), as well as the outer and inner diameters of the tubular fiber (g, h).

The following conclusions can be drawn:

- As the thickness of the sample (fiber length) increases, the phase difference changes due to an increase in the path passed by light inside the fiber and an increase in the number of reflections.
- The axis of symmetry of the fibers is perpendicular to the plane of the sample. The interference pattern will have the form shown in figure 2 c d and if the axis of symmetry will have an inclination with respect to the plane of the sample, then the interference pattern will take the form shown in figure 2 e f.
- The axis of symmetry of the fibers is inclined to the plane of the sample. With an increase in the outer diameter of the fiber tube (the inner diameter is constant), there is a decrease in the number of interference rings and an increase in their thickness due to a decrease in the number of light reflections inside the fiber as the wall thickness of the tubular fiber increases (Figure 2 g, h).
- The axis of symmetry of the fibers is inclined to the plane of the sample. If the outer diameter of the tube is constant and the inner diameter decreases, the number of interference rings decreases and their thickness increases.

Waveguide model

The description of the transport of light in the radial approximation is quite clear and allows us to study the general patterns of distribution of light beams in relatively thick anisotropic light-guides isolated from each other light-microcapillaries distributed according to the laws of axial symmetry [8,25-28]. However, with the close packing of such microcapillaries, and most importantly with their cross-sections comparable to the wavelength, it is required to use waveguide methods for describing the transport of light in such systems.

Mathematical modeling of light propagation in an inhomogeneous medium for a composite structure consisting of a set of closely spaced mutually parallel tubes is presented in the work [29]. The properties of biotissue, similar in their optical and physical parameters to the dentin of the tooth, which is an ordered set of microcapillaries - dentin tubes located in the intertubular dentin, are modeled.

The purpose of mathematical modeling is to substantiate the light effects observed during the transport of polychromatic light through a thin slice of dentin. The calculation makes it possible to distinguish individual trace elements of the structure of the biotissue and, therefore, provides the observation of a characteristic interference pattern localized on the surface of the cut in any part of the grind. The calculation of such a picture and its visual display on a computer is possible with the involvement of the wave theory of light, although in this case the well-known models of Kirchhoff, Fraunhofer and Sommerfeld, based on the solution of the paraxial wave equation, are insufficient.

In the work [29] it is proposed to use a general approach, which uses a numerical solution of a heterogeneous wave equation. In the works [29] such solutions are considered in relation to single fiber-optic nanoprobes and micropipets. For the purposes of this study, it is important to apply these solutions in structures consisting of several, and in general many dozens of microcapillary tubes. If for single dielectric tubes it is possible to use solutions in the form of waveguide modes, then in this case this approach encounters the difficulties of joint calculation of the field in all tubes at once, when any points of a given structure are interrelated in terms of the distribution of the complex amplitude of the field. Applying waveguide theory would require an extremely large amount of computation, which is almost impossible due to the large amount

of computation. At the same time, the numerical solution of the wave equation on the basis of the approach outlined in the works [29], but in relation to several tubes located in a certain dielectric medium, opens up the possibility of analyzing the passage of light through such composite «multicellular» structures. The program is a Windows-based application written using the object-oriented MFC library, the discrete two-dimensional Fourier transform block is built on the basis of the functions of the adaptive library FFTW 2.1.3., developed at MIT (Massachusetts Institute of Technology), which made it possible to several times increase the speed of calculations. The program allows you to calculate the light distribution over the entire volume of the structure, as well as in the air in the small vicinity of the lower end of the grind.

The structure of the grind, through which it is necessary to investigate the transport of light, is determined for the program by specifying geometric and optical parameters. Thus, the tooth dentin is characterized by the following values: the dielectric constants of the matrix (intertubular dentin), the membranes and cores of the waveguides (dentin tubes) are 2.25, 2.65 and 1.77, respectively, the radii of the shell and the cores of the waveguides-tubes are in the ranges (0.5-1.75) μm and (0.2- 0.75) μm respectively, and the distance between the axes of waveguides is $\sim 4 \mu\text{m}$. In addition, to create a more adequate and complete model of the biotissue under consideration, the program provides for the possibility of modeling inside the wall of the tubes the inclusions of MICROCRYSTALS of HAP having a habitus of parallelepipeds, which are separated by a thin layer of organic matter.

When modeling dentin tissue in order to simplify the calculations, certain assumptions were made [30,31]. For example, it is assumed that the light-guide tubes are mutually parallel at the entire depth of the structure, while it is known that in dentin a bundle of dentin tubes is an axisymmetric truncated cone with a slight angular opening [8,26]. The next assumption is that in the model representation, the light-guide tubes have a uniform hexagonal distribution over the volume of the structure. Considering the optical-physical parameters of the simulated composite medium, it should be noted that when calculating the absorption and scattering values of the media are taken to be zero, the dispersion properties of the media and the birefringence of the light-guide tubes are also not taken into account in this program. As an example, Figure 3 shows a variant of the cross-section of the structure synthesized by the program.

Figure 3: Cross-sectional model of the structure.

Figure 4 shows a picture of the relative intensity distribution calculated for a structure composed of sixteen light guides (the cross-section of this structure is conventionally depicted in Figure 3). The planes for which the light distribution is calculated pass through the axes of the light guides-tubes, the trace of this plane is depicted in figure 4 light intermittent line. Incident radiation is represented by wavelengths: 400, 550 and 700nm. As can be seen from the figure, most of the radiation energy is localized in the volume of the shell of light guides, and the radiation penetrates into the core only to a depth of about 3-4 μm . *This fact agrees well with the experimental data and corresponds to the features of the phenomenon of total internal reflection (TIR), since the refractive index of the shell exceeds the indicators of the core and matrix.*

Figure 4: Calculation. The relative distribution of intensity in the vertical section of the structure.

From figure 4 clearly shows that the light field, depending on the wavelength, propagates along the shells of the light-guides in different ways, but nowhere does it penetrate the core. The most characteristic similarity between the calculation and the experiment performed on a microscope in crossed polarizers [4,6] is observed when comparing them, from which a correlation of a peculiar color is revealed when light propagates along the tubes located in the plane of horizontal tooth grinding, see figure 5.

Figure 5: Experiment. A photograph of a fragment of a section of a molar tooth obtained on a microscope in crossed polarizers: a-frame size 150×150 μm . Dentinal tubules are visible, which are in the vicinity of the DES and are located at an oblique angle to the surface of the section (lower left). This part of the tubules has an intense color. In the upper part of the photo of the tube, parallel to the surface of the thin section (above). The color of this part of the tubes is less intense. b- Frame size 15×20 μm , taken from the a-top of the photo. Tubes are visible parallel to the section in separate area painted in green and red.

The pearl coloration of the tubes, formed by micro-glare of dark green and red-brown color, as can be seen from the photograph, changes continuously along the length of the tubes. The blue color in the experiment is practically absent, apparently due to the Rayleigh scattering of short wavelengths. The center of the tubes is dark and their ends glow brightly. Moreover, the color of the ends of neighboring tubes is different, there are areas where the tubes are bright white, i.e. do not have a colored color. However, there are areas with intense coloration of the ends. This color is predominantly dark green and red-brown, occasionally found in the picture tubes of dark blue color, see figure 5. It is significant to note that the microscope illuminator was an ordinary incandescent light bulb. When the tubes are illuminated with white light of

different colors, the rays during their transportation inside the fiber with the help of internal reflection will pass through sections of the fiber of different lengths along the path. This effect is enhanced for dispersion for different wavelengths and birefringence.

It should be noted that the field distribution calculated specifically within a single light guide and in a small neighborhood from it differs very slightly from the field distribution inside any light guide of several that make up the structure. However, outside the light-tubes, the field distribution is different in the case of one or more light guides. This suggests that the propagation of the field in the structure with the specified parameters is influenced by all the light guides. Comparison of the calculation with the experiment shows that in the dentin there are areas where the axes of the tubes are located at distances <2 diameters. At such distances, for tubes located perpendicular to the plane of the grind, the pumping of light energy between closely spaced tubes-light guides is experimentally well observed. This pumping is manifested in the form of light jumpers between the closely spaced ends of the tubes that come to the surface of the grind, see figure 6. The data obtained agree well with the calculations for glass light guides located at the same distance from each other [32].

Figure 6: a - Calculation. Relative distribution of intensity in the cross-section of the structure. b - A photograph of a fragment of the grinding of a molar tooth, obtained on a microscope in crossed polarizers. Frame size $20 \times 20 \mu\text{m}$. The zone is characteristic in the form of a cross - light bridges between the luminous ends of 4 dentin tubes are visible.

For comparison, Figure 6b shows an experiment for a local grinding site. Figure 6b clearly shows the glow of the ends of 4

tubes and the features of the distribution of the glow at the ends and between them, which confirms the possibility of pumping light energy between the tubes.

Interference-polarization method of research and equipment

Preliminary studies have shown that standard optical polarization equipment (POLAM model microscope) is not suitable for the survey diagnosis of grinds, since in this case it is desirable to have a small magnification (3-5 times), but a large field of view. Therefore, a device was developed and manufactured, on which part of the interference-polarization studies of tooth grinds was performed.

A more detailed analysis of dentin plots, which were previously visualized using the above equipment, were then additionally studied on optical microscopes with polarizing devices at high magnification. The object (grinding) was in a special chamber with constant humidity. Under certain lighting conditions (light falls along the axis of the tubes), the matrix plays the role of a scattering medium, and the tubes play the role of light guides. At the same time, the optical image formed by such a system at low magnification is perceived by the observer in the form of a picture that is formed in the form of mosaic local "points" that are the ends of the tubes. The state of polarization of a separate local "point" of the observed picture characterizes the optical properties of this tube, its dimensions (diameter, length, surface micro-relief, etc.) and its direction in the grind.

Studies of the topography of dentin tubes in the tooth grind

The model approach was used in the selection of grinders that meet the results of the calculation to the greatest extent - the presence of a system of interference rings of different shapes. Such samples were soon identified from a batch of polished grinders of molars and premolars (thickness 0.5-1 mm), a total of 36 polishes of human and pig teeth, Molars of domestic pigs are an interesting system for studying the process of biomineralization. The large size, thick enamel and complex morphology of the crown make the molars of pigs relatively similar to human molars. However, compared to human molars, the molars of pigs develop significantly. However, compared to human molars, the molars of pigs develop significantly.

It is established that some of the studied grinds are well described using the geometric optical model discussed above.

The model made it possible to interpret from a single position the appearance of qualitatively different experimental interference-polarization patterns formed in the grindings of a human tooth and a pig. At the same time, the revealed details of interference-polarization patterns in the pig tooth were qualitatively well described by model calculation, but for other model parameters (the number of local zones, with an ordered structure of the tubes, the inclination of the axis of the bundle of tubes, the angle of the alignment of the bundle of tubes). The biological causes leading to the difference in the observed interference-polarization patterns of human and pig tooth grinds are considered.

Distribution of tubes in the center of the grinder

The results of interference-polarization studies of grinding are considered. Attention is drawn to the bright colorful picture in the enamel layer, formed in the transmitted light of most samples. The color bright picture of red and green spots and stripes in the enamel layer is associated with the interference of polarized rays in a crystalline medium.

The most interesting results were obtained for grinding molars and premolars cut in a horizontal section between the pulp and crown of the tooth, figure 7.

Figure 7: Above. Photo of molar (left) and premolar. Below. Enlarged fragments of local zones: on the left-molar (4 zones) and on the right-premolar (1 zone). Observational conditions: the main sections P and A are deployed in relation to each other by 90° degrees.

The entire grinding was observed, with the dentin region adjacent to the DES looking like a dark border, and the four rounded corners of the grind on a gray background show bright glowing circles near the border of the DES, inside of which dark symmetrical figures are clearly distinguished, mainly like crosses. In some specimens, a large dark, weakly contrasted cross surrounded by dark concentric circles was seen in the center of the grind. The described picture is observed on a light background due to diffuse scattering of the organic matrix. It is noticed that the crosses are located near the protrusions or rounded corners of the sagittal grinds. The appearance of the described figures indicates a high orderliness of the tooth structure in the vicinity of the crown.

The structural elements responsible for the appearance of the described figures are tubes that fan out from the center of the tooth in the direction of the DES. This orientation of the tubes, which play the role of light guides, leads to a dark framing strip near the DES when illuminating the plate from the upper plane of the grind. The low contrast of the large cross in the center, which could only be observed for individual young teeth, and the relatively high contrast of the small crosses is associated with a denser distribution of tubes in the unit area in the area where the crosses are located.

The dentin structure in the center of the horizontal cross-section grinding exhibits the properties of a single-axis crystal with an optical axis oriented perpendicular to the cross-section of the grind. When illuminating the grinding, light propagates through the tubes as if through waveguides and in the place of their increased density on the unit. area, brighter areas are observed, Figure 8.

Figure 8: Diagram of the indicatrix of brightness in the local zones of the grinding of the molar when observed from the plane P1. The grinder is illuminated from the side of P2. Observational conditions: the main sections P and A are deployed in relation to each other by 90° degrees.

Such bright areas are characteristic of areas where crosses are visible. At the same time, from Figure 8 shows that the brightness indicatrixes in the region of the zones of the small crosses have an inclination and their axes intersect at a point that is in the region of the pulp. In some specimens, a large dark weakly contrast cross (or fragments of it) was visible in the center of the grind, see Figure 9 (concentric rings are not shown in the diagram). The dentin structure in the center of the grind, where the cross is observed, exhibits the properties of a uniaxial crystal with an indicatrix perpendicular to the plane of the grind. The structural elements responsible for the appearance of the described figures are tubules, which in a symmetrical fan diverge from the center of the tooth in the direction of the DES. The low contrast of the large cross in the center, which could only be observed for single samples of grinding, and the relatively high contrast of the small crosses is associated with a denser distribution of tubes in the unit area in the zone where the crosses are located. Electrometric studies performed on grinds also show a decrease in electrical resistance in areas where crosses are observed [12].

Structural organization of tubules near the dentino-enamel layer

Interference patterns observed near the dentino-enamel layer (DES) show the difference in the location of the tubes in this zone from their orientation in the center of the grinding. Near the DES, the tubules are oriented perpendicular to the DES, i.e. lie in the plane of the grind. A dark line was found separating the central part of the grind and the wall part bordering the DES, see figure 8. The thickness of this line (≈ 0.2 mm) is calculated, its optical properties (isotropic) and the distance from the DES ($\approx 0.2-0.5$ mm). Between this dark line and the DES, the tubes are located mainly in the plane of grinding or (more precisely) make up a small angle of α with the plane of grinding. This area, when observing the grinding from above, stands out as a dark border adjacent to the DES, see figure 7. When observed at angles $\alpha = 60-80^\circ$, the brightness of this border becomes comparable to the brightness of the center of the grind when observed near the angle of $\alpha = 0-10^\circ$.

The obtained data concerning the orientation of the tubes near the DES are confirmed by additional color measurements [23] on the instrument [27], using a standard phase-sensitive plate included in the set of the POLARIZATION MICROSCOPE POLAM. Figure 9 presents a measurement scheme using a phase-sensitive (FP) plate.

Figure 9: Scheme of observations with FP plate. Designations: on the left - the light vector E, o. o.-optical axis of the fiber (tubes); in the center - color fields for different orientations of the fiber in the grind and vector E; on the right - the scheme of the observed picture for the molar.

On the left in the margins of the figure, the orientation of the electric light vector E and the direction of the optical axis (o. o.) of the anisotropic object are indicated, in the center the color fields (1-gray-steel, 2-blue-green, 3-yellow) are shown, which appear with the appropriate orientation of the object, analyzer A and polarizer P. On the right, the general scheme of the grinding (in color form) is shown, which the observer sees in the field of view of the device. The steel-gray color indicates that there is practically no difference in travel between the interfering rays. This result directly confirms the perpendicular arrangement of the tubes in the center of the grind. When the object is turned at an angle of $\theta = 90^\circ$, the colors of fields 2 and 3 mutually change. The same color at the edges of the grind and in local zones (the cross zone) indicates a close difference in the optical course of interfering rays at the output of analyzer A, which is in a crossed position with respect to the polarizer P.

Distribution of tubules and their organization in local areas of the tooth

When illuminating the grind from the side of the plane P_2 , see Figure 1, it is established that the optical axes of all local light guides converge in some small region located under the plane P_1 . This area in its position coincides with the region of the pulp of the tooth [25,28]. The direction of the light guides in the opposite direction from the pulp will coincide with the area of the centers of the tubercles of the crown of the tooth. It is shown that the increased brightness of these zones in relation to the background is associated with a greater density tubes in the area of these zones.

It has been established that the number of local light-guide channels (formed by a set of tubes) in a particular tooth is determined by the number of tubercles on the crown. It is noticed that as the studied horizontal grinds shift in the direction: molar - premolar - canine - incisor, the number of main local light channels decreases to one. As an example, we can compare typical photos of a molar and a premolar, see figure 7.

Studies on a microscope made it possible to establish the fractal nature of the structure of dentin. The structural organization of tubes similar to that where crosses are observed was also found in separate local areas of grinding in the form of zones $\approx 0.01 \div 0.05$ mm, formed by a small set of tubes.

Electrometric measurements of the crown part of the tooth

An independent electrometric method was used to verify the data obtained by the optical method. The use of a special experimental installation for research makes it possible to measure the ohmic resistance of the tooth grind under study at individual local points that can be obtained by scanning from its entire surface. In accordance with the developed measurement methodology, manual scanning made it possible to obtain data on a set of grinds, which allow to form an objective idea of the structure of the grinds from the point of view of electrometric measurements [33,34]. To visually represent the change in resistance on the surface of the grind as a result of the experiment, Figure 10 shows the experimental data for different scales of change in resistance along the Z axis.

Figure 10: Results of electrometric measurements of tooth grinding resistance. In the center, 4 zones of reduced electrical resistance are visible. Intense red coloration in the local area means reduced resistance. At the top is a photo of a molar slyph obtained in crossed polarizers.

Comparison of the results of the calculation and the experiment leads to the following conclusions:

The obtained physical and mathematical model corresponding to the structure of solids the tissues of the teeth, within the framework of the experiment, coincide with optical data.

The electrical resistance of the tooth tissues depends on the structure of the capillaries, lowering the dentin of the tooth and providing, apparently, nutrition to the hard ones dental tissues.

Electrical resistance increases as you move from the center of the distributor. Odontoblasts to the periphery of the tooth, which is fully consistent with the theoretical tooth models.

The nutrition of the hard tissues of the teeth depends on the distribution of capillaries in the dentin and is carried out more intensively through the so-called tooth growth points, respectively, the following mounds of enamel located on the crown of the tooth. The experimentally and theoretically revealed structure of the hard tissues of the tooth on Based electrical sensing signal correlates with a similar structure a swarm obtained through the use of an optical sounding signal.

The results obtained confirm that the optical model correctly describes the optical properties of local zones of real grinding (local dentin zones). Thus, it is shown that the method of modeling optical properties in local grinding zones has a prognostic value and makes it possible to interpret the type of experimental interference-polarization patterns formed in the grindings of a human tooth and a number of animals. Biological considerations are expressed about the reasons for the discrepancy between the interference-polarization patterns of individual grinds and the results of the calculation.

Thus, it was established that dentin in its crown region has a more complex structure than previously thought in the special optical and biological literature.

Classification of the organization of tubules in the crown part of the tooth

On the example of the study of interference-polarization patterns for molars, the correlation of the optical properties of local zones with crosses (brightness, size of the cross) with the shape and size of individual tubercles of the crown of the human and animal tooth was established [28]. On this basis, a classification of the types of distribution of tubules in the dentin of teeth of different types is carried out. Three classes of structural organization (distribution) of tubes in dentin have been allocated, see figure 11.



Figure 11: Scheme of distribution of tubes for molars: a- Uniform, b- Monodirectional, c- Tree-shaped. Arrows show the axes of the tube bundles.

The type of uniform distribution of tubules, given in figure 11a, most corresponds to the traditional ideas of modern biological literature. However, in practice, we have more often encountered cases presented in figure 11 b, c. Types of distribution of tubes in the dentin of the tooth, presented in figure 11, are manifested when considering such objects for horizontal grinding in the form of local zones with crosses, the brightness and size of the zones increase as you follow from figure 11a in the direction of figure 11c. The nature of the distribution of tubes in the dentin is reflected in the formation of the features of the shape and relief of the structure of the tooth crown. For samples, presented in figure 11a, the shape of the crown and the smooth layer of crown enamel are most consistent with the existing ideas about the «norm» in the biological literature [7]. For the samples shown in figure 11b, the tubercles are more prominent and the tubes are deeply embedded in the enamel layer, sometimes coming to its surface. In the case of figure 11c, bulges form on the surface of the crown, bulges form in those areas where the tube bundles fit. This indicates that the tubes for samples having a distribution according to the type figure 11b are located in a wider corner alignment. In some specimens, fragments of a large dark cross surrounded by dark concentric circles were seen in the center of the grind. The cross and the dark rings around the cross were weakly contrasty, which is probably due to the low density of the distribution of tubes in the unit area and their fan type of opening. This type of opening of the tubes leads to the inclination of the indicatrix of the brightness of the light beam in relation to the surface of the grind. As a result, the brightness of the radiation coming out of the tubes in relation to the surface of the grind will be much lower than in the case when the tubes are organized into structures of the cone type with a small angle of the leaf.

These data indicate the important role of the structural organization of the distribution of dentin tubes at the stages of growth and formation of the shape and relief of the crown part of the tooth. The data obtained confirm the well-known biological rule - «the function of a biological organ is reflected in its structure.» Tubes at the stage of tooth growth perform the function of traffic (nutrition) of the biotissue, and at the stage of a mature tooth - a function that provides mechanical strength and stiffness of the tubercles-tops of the crown of the tooth. A large axial load on the base of the molar tooth (molar tooth) is transmitted in the process of grinding food, in this process this tooth acts like a ball mill. Therefore, at the first stage of the formation of a young tooth, i.e. at the growth stage, the tubules have thin walls of pertubular dentin and a relatively large diameter of the internal channel through which traffic is carried out, at the second stage, the diameter of the internal channel decreases due to the growth of the wall thickness and, accordingly, the mechanical strength and stiffness of the tubes increases.

Comparison of the shape of the crown of the tooth of the human molar and a number of mammals

Analysis of the morphology of the tooth of the human molar and a number of herbivorous mammals shows noticeable systemic differences in the shape of their crown. The closest in shape is the tooth of the pig, but it is an omnivore and herbal food is not the main one in its diet. Despite the similarity of the crown of the molar of the pig and human tooth, significant differences in the morphology of the crown are noticeable. In humans, the tubercles of the crown are more rounded and their relief is smoothed [7], Figure 12.

Figure 12: Drawings and photos of molars of a number of animals The human tooth is shown in the top row on the right (not signed).

On the surface of the pig molar there are many local prismatic sharp protrusions with dimensions of about 0.5-1 mm. Therefore, the picture of the pig tooth for optical measurements of the grinding points to a large number of zones in the form of small crosses, large crosses, characteristic of the grinding of the human molar, are not characteristic of the grinding of the pig. This is due to the more complex organization of the structure of the tubes in the crown zone of the pig molar. This shape of the tooth is designed for crushing and grinding food. In its own way, the pig's molar it resembles a sharp grater [35-38].

The change in the shape of the crown of the tooth is clearly seen in the analysis of herbivorous mammals. As the size and mass of the animal increases, the shape of the tooth begins to transform - the fossa in the center of the tubercles expand and from rounded become elongated. This trend intensifies as the animal's mass increases. For example, for an elephant and a mammoth, the bridges between the pits turn into a series of extended enamel strips, representing elongated tubercles. The number of stripes increases with the size of the animal. Each strip consists of two adjacent extended protrusions of low height, Figure 12. This shape of the tooth is most adapted for effectively grinding a large amount of food.

Use of the obtained data for forecasting and diagnosis of dental diseases

The proposed method of studying the grinds and the considered classification of the organization of dentin tubes made it possible to identify some correlations between the thickness of the enamel and the relief of the crown of the tooth, depending on the type of organization of the dentin tubes. The data obtained are consistent with the hypothesis of the efferentia [9] of nerve fibers, see Figure 1b, which go inside the walls of dentin tubes adjacent to the pulp zone [9], and thus explain the reason for their greatest concentration in local zones grinding (the zone of crosses), and as a consequence of their influence on the growth and formation of the crown of the tooth.

The mechanism of structural organization of tubules in local areas near the pulp horns can be explained in terms of the efficiency of nerve fibers that transmit a "signal" from the pulp area of the tooth and control tooth growth. Fibers of another type - afferent fibers perceive the "signal" as a result of a change in their environment [7]. It has been shown that the nerve fibers in the dentinal tubules,

Bibliography

1. Zijp JR and ten Bosch JJ. "Theoretical model for the scattering of light by dentin and comparison with measurement". *Applied Optics* 32.4 (1993): 411-415.
2. Zijp JR and Ten Bosch JJ. "Angular Dependence of HeNe-Laser Light Scattering by Bovine and Human Dentine". *Archives of Oral Biology* 36.4 (1991): 283-289.
3. Altshuler GB and Grisimov VN. "The effect of waveguide propagation of light in the human tooth". *Reports of the Academy of Sciences of the USSR* 310.5 (1990): 1245-1248.
4. Grisimov V.N. "Refractive index of bulk dentin". *Advanced Laser Dentistry: Proc. SPIE*. 1984: (1994) 2-5.
5. Zolotarev V M and Grisimov VN. "Architectonics and Optical Properties of Dentin and Dental Enamel". *Optics and Spectroscopy* 90.5 (2001): 753-759.
6. Walton RE., *et al.* "Magnification - An Interesting Optical Property of Dentin". *Journal of Dental Research* 55.4 (1976): 639-642.
7. Bykov VL. "Histology and embryology of organs of the human oral cavity". SPb.: Spets. literature, (1999): 247.
8. Zolotarev VM. "Light interference in composite systems based on ordered anisotropic fibers. Part 1. Physical Foundations". *Journal of Optical Technology* 69. 3 (2002): 10-14.
9. Zhevandrov ND. "Polarization Physiological Optics". *Uspekhi Physical Sciences* 165.10 (1995): 1193-1225.
10. Tuchin VV. "Research of biotissuaries by methods of light scattering". *Successes of Physical Sciences* 167.5 (1997): 517-539.
11. Lopatin VN and Sidko FYa. "Introduction to the optics of cell suspensions". Novosibirsk. Nauka, (1988).
12. Muller G., *et al.* "Medical Optical Tomography: Functional Imaging and Monitoring". (Bellingham: SPIE, 1993) IS11.
13. Roggan A. *et al.* In: "Cell and Biotissue Optics: Applications in Laser Diagnostics and Therapy". (Bellingham: SPIE, 1994) 2100. 42.
14. Boyde A. "Enamel". In: Berkovitz B.K.B., Boyde A., Frank R.M. *et al.* "Teeth". Berlin, etc.: Springer-Verlag. (1989): 309-473.

15. Borovsky EV and Leontiev VK. "Biology of oral cavity". *Medicine* (1991): 302.
16. Jernvall J and Thesleff I. "Reiterative signaling and patterning during mammalian tooth morphogenesis. Mechanisms of Development". 92.1 (2000): 19-29.
17. Berkovitz BKB, *et al.* "A Color Atlas and Textbook of Oral Anatomy". London. Wolfe Med. Publ. Ltd. (1978).
18. Freid D., *et al.* "Nature of light scattering in dental enamel and dentin at visible and near-infrared wavelengths". *Applied Optics* 34.7 (1995): 1278-1285.
19. Wang Xiao-Jun., *et al.* "Characterization of dentin and enamel by use of optical coherence tomography". *Applied Optics* 38.10 (1999): 2092-2096.
20. Vaarkamp J and Ten Bosh JJ. "Propagation of light through human dental enamel and dentine". *Caries Research* 29.1 (1995): 8-13.
21. Kislovsky LD., *et al.* "Signs of condensation of tetrahedra in the structure of apatite". *Dokl. AN SSSR*, 232.3 (1977): 581-583.
22. Odor TM., *et al.* "Effect of probe design and bandwidth on laser Doppler readings from vital and root-filled teeth". *Medical Engineering and Physics* 29.4 (1996): 228-234.
23. Shubnikov AV. "Fundamentals of optical crystallography". M. Izd. AN SSSR, (1958): 205.
24. Landsberg GS. "Optics". *Science* (1962): 926.
25. Kozhukhov SS., *et al.* "Modeling of optical properties of composite structures based on anisotropic fibers with axisymmetric stacking". *Journal of Optical Technology* 70.1 (2003) 12-17.
26. Zolotarev VM., *et al.* "Part 2. Optical studies of the influence of the structural organization of dentin tubes on the structure and shape of the tooth crown". *Journal of Optical Technology* 69. 3 (2002): 15-20.
27. Zolotarev VM. "Optical properties of composite systems based on anisotropic fibers with axisymmetric stacking". *Optics and Spectroscopy* 97. 4 (2004): 696-703.
28. Zolotarev VM., *et al.* "Optical technologies in fundamental and applied research". Sb. articles ed. V.N. Vasilyev, SPb IFMO, St. Petersburg, (2001).
29. Voznesensky NB. "Optimum choice of basic functions for modeling light propagation through nanometer-sized structures". *Proc. SPIE*. 3791 (1999): 147-157.
30. Voznesensky NB. "Mathematical modeling of the processes of propagation and diffraction of light in nanostructures". Sb.materials Vseros. talk. "Probe microscopy-2000", Nizhny Novgorod. February 28-March 2, (2000): 142-146.
31. Voznesensky NB., *et al.* "Scalar modeling of light propagation in multi-wave structures". *Journal of Optical Technology* 70.1 (2003): 6-11.
32. Traps N. "Voloconnaia optika". *Peace* (1969): 464.
33. Ivanova GG., *et al.* "Comparative analysis of the study of dental dentin by X-ray and electrometric methods". *Institute of Stomatology* 1.22 (2004): 94-99.
34. Tikhonov EP. "Micro- and macromorphology in the formation of the genesis of hard tissues of the tooth". *Institute of Stomatology* 2.27 (2005): 73-77.
35. Zolotarev VM. "Visualization of adaptive growth centers that form the crown of a human tooth". Scientific and technical. vestnik SPb IFMO, ed. V.N. Vasilyeva. 21 (2006).
36. Sova SS., *et al.* "A microCT Study of Three-Dimensional Patterns of Biomineralization in Pig Molars". *Frontiers in Physiology*. Sec. Craniofacial Biology and Dental Research 9 (2018).
37. "Identifying common animal bones from archaeological sites: a brief introduction".
38. Fortelius M. "Ungulate cheek teeth: developmental, functional, and evolutionary interrelations". *Acta Zool. Fennica*, 180 (1985): 1-76.